Available online at www.sciencedirect.com
ScienceDirect
Journal of Hazardous Materials 147 (2007) 792–799
Journal of Hazardous Materials
www.elsevier.com/locate/jhazmat

Fast removal of copper ions by gum arabic modified magnetic nano-adsorbent

Shashwat S. Banerjee, Dong-Hwang Chen *

Department of Chemical Engineering, National Cheng Kung University, Tainan 701, Taiwan

Received 26 September 2006; received in revised form 6 January 2007; accepted 8 January 2007
Available online 26 January 2007

Abstract

A novel magnetic nano-adsorbent was developed by treating Fe_3O_4 nanoparticles with gum arabic to remove copper ions from aqueous solutions. Gum arabic was attached to Fe_3O_4 via the interaction between the carboxylic groups of gum arabic and the surface hydroxyl groups of Fe_3O_4. The surface modification did not result in the phase change of Fe_3O_4, while led to the formation of secondary particles with diameter in the range of 13–67 nm and the shift of isoelectric point from 6.78 to 3.6. The amount of gum arabic in the final product was about 5.1 wt%. Both the naked magnetic nanoparticles (MNP) and gum arabic modified magnetic nanoparticles (GA-MNP) could be used for the adsorption of copper ions via the complexation with the surface hydroxyl groups of Fe_3O_4 and the complexation with the amine groups of gum arabic, respectively. The adsorption rate was so fast that the equilibrium was achieved within 2 min due to the absence of internal diffusion resistance and the adsorption capacities for both MNP and GA-MNP increased with increasing the solution pH. However, the latter was significantly higher than the former. Also, both the adsorption data obeyed the Langmuir isotherm equation. The maximum adsorption capacities were 17.6 and 38.5 mg/g for MNP and GA-MNP, respectively, and the Langmuir adsorption constants were 0.013 and 0.012 L/mg for MNP and GA-MNP, respectively. Furthermore, both the adsorption processes were endothermic due to the dehydration of hydrated metal ions. The enthalpy changes were 11.5 and 9.1 kJ/mol for MNP and GA-MNP, respectively. In addition, the copper ions could desorb from GA-MNP by using acid solution and the GA-MNP exhibited good reusability.

Keywords: Nanoparticle; Magnetic; Gum arabic; Adsorption; Copper ions

1. Introduction

The environment and all the life on earth face a very serious threat as a result of heavy metal pollution due to rapid industrialization and the increase in the world population. Unlike organic pollutants, the majority of which are susceptible to biological degradation, metal ions do not easily get converted into harmless end products. The metals that cause serious concern include Cr, Hg, Cu, Ni, Zn and Cd, which are commonly associated with pollution and toxicity problems [1].

Many processes have been developed to curtail heavy metal pollution, including chemical precipitation, electrode deposition, solvent extraction, ion-exchange, activated carbon adsorption and biological methods [2,3]. Among these methods, adsorption has increasingly received more attention in recent years because it is simple, relatively low-cost, and effective in removing heavy metal ions from wastewaters [4].

Nanotechnology has been considered as one of the most important advancements in science and technology. Its essence is the ability to fabricate and engineer the materials and systems with the desired structures and functionalities using the nano-sized building blocks [5]. Nanoparticles are one of the important building blocks in fabrication of nanomaterials. Their basic properties, extremely small size and high surface-area-to-volume ratio, provide better kinetics for the adsorption of metal ions from aqueous solutions. However, for such an application, it is necessary to use a method of purification that does not generate secondary waste and involves materials that can be recycled and easily used on an industrial scale [6].

Magnetic separation has been shown to be a very promising method for solid–liquid phase separation technique. To facilitate the recovery and manipulation of nanoparticles, magnetism is incorporated with the nanoparticles. This makes magnetic nanoparticles excellent candidates for combining metal binding

* Corresponding author. Tel.: +886 6 2757575x62680; fax: +886 6 2344496.
E-mail address: chendh@mail.ncku.edu.tw (D.-H. Chen).

0304-3894/$ – see front matter © 2007 Elsevier B.V. All rights reserved.
doi:10.1016/j.jhazmat.2007.01.079

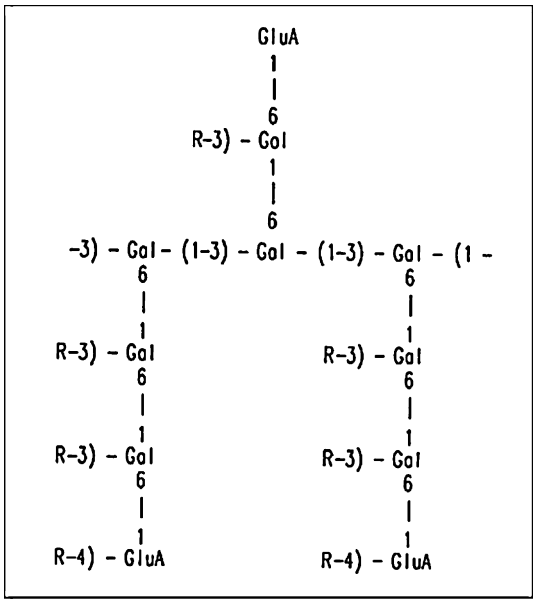

Fig. 1. Structure of gum arabic.

and selective adsorption properties with ease of phase separation [7]. Numerous types of magnetic nanoparticles for various applications could be tailored by using functionalized natural or synthetic polymers to impart surface reactivity. In this work, a novel magnetic nano-adsorbent was developed for the adsorption of metal ions by the surface modification of Fe_3O_4 nanoparticles with gum arabic (Fig. 1), which is a natural, harmless and environment friendly polymer containing active functional groups like carboxylate and amine groups [8,9]. The size, structure, and surface properties of gum arabic modified magnetic nanoparticles (GA-MNP) were characterized by transmission electron microscopy (TEM), X-ray diffraction (XRD), zeta potential meter, dynamic light scattering (DLS), Fourier transform infrared (FTIR) spectroscopy, and thermogravimetric analysis (TGA). The adsorption capability was demonstrated using copper ions as the model metal contaminant because of their extensive environmental impacts as well as strong Lewis acid characteristics. The adsorption behavior and mechanism were investigated and compared to those for the naked Fe_3O_4 magnetic nanoparticles (MNP).

2. Experimental

2.1. Materials

Ferric chlorides, 6-hydrate was purchased from J. T. Baker (Phillipsburg). Ferrous chloride tetrahydrate were purchased from Fluka (Buchs). Ammonium hydroxide (29.6%) was supplied by TEDIA (Fairfield). Gum arabic was purchased from Fluka (Buchs). Copper nitrate was obtained from Riedel-deHaën (Seelze). The water used throughout this work was the reagent-grade produced by a Milli-Q SP ultra-pure-water purification system from Nihon Millipore Ltd., Tokyo. All other chemicals were of analytical grade and used without further purification.

2.2. Fabrication of gum arabic modified magnetic nanoparticles

Fe_3O_4 nanoparticles were prepared by coprecipitating Fe^{2+} and Fe^{3+} ions with ammonia solution and treating under hydrothermal conditions according to our previous work [10,11]. The ferric and ferrous chlorides (molar ratio 2:1) were dissolved in water at a concentration of 0.3 M iron ions. Chemical precipitation was achieved at 25 °C under vigorous stirring by adding NH_4OH solution (29.6%). During the reaction process, the pH was maintained at about 10. The precipitates were heated at 80 °C for 30 min, then washed several times with water and ethanol, and finally dried in a vacuum oven at 70 °C.

For the surface modification with gum arabic (GA), 1.0 g of Fe_3O_4 nanoparticles were added into 100 mL of gum arabic solution (5 mg/mL) in a stoppered bottle. The reaction mixture was sonicated for 20 min and then mixed on a vortex mixer for 5 min and again sonicated for another 10 min. The resultant gum arabic modified magnetic nanoparticles were recovered from the reaction mixture by placing the bottle on a permanent magnet with a surface magnetization of 6000 G. They settled within 1–2 min, then were washed three times with 100 mL of water, and finally dried in an air oven at 50 °C for 24 h and stored in a stoppered bottle for further use.

2.3. Characterization

TEM analysis was carried out using a Hitachi Model H-7500 at 120 kV. The sample was obtained by placing a drop of colloid solution onto a Formvar-covered copper grid and evaporated in air at room temperature. XRD measurement was performed on a Rigaku D/max III.V X-ray diffractometer using Cu Kα radiation ($\lambda = 0.1542$ nm). FTIR spectra were recorded on a Varian FTS-1000 FTIR spectrometer. The zeta potentials were measured on a Malvern ZEN2600 Zetasizer Nano Z. The hydrodynamic diameter was measured by dynamic light scattering using a Malvern Autosizer 4700/PCS100 spectrometer equipped with an Ar ion laser operating at 488 nm. TGA was done on the dried samples in air with a heating rate of 10 °C/min on Shimadzu TA-50WSI TGA.

2.4. Adsorption and desorption studies

The adsorption of copper ions by the magnetic nano-adsorbents (MNP or GA-MNP) was investigated in aqueous solutions at pH 2–6 and 300–340 K. In general, 25 mg of magnetic nano-adsorbent was added to 5 mL of copper nitrate solution. After mixing by a shaker (200 rpm) for 5 min, the magnetic nano-adsorbent was removed magnetically from the

solution. The solution pH was adjusted by NaOH or HCl. The concentrations of copper ions were measured using a GBC Avanta Atomic Absorption Spectrometer. Unless otherwise specified, the absorption experiments were performed in aqueous solution at pH 5.1, 300 K, and an initial copper ion concentration of 200 mg/L. Each experiment was repeated twice and the reproducibility was found to be fairly good. The error percentage was within 3%.

Desorption of copper ions was studied by placing 25 mg of copper ions-loaded GA-MNP (prepared by shaking 25 mg of GA-MNP with 5 mL of 200 mg/L of copper nitrate solution for 5 min at pH 5.10) in 5 mL of HCl solutions (3.0, 2.0 or 1.5). After stirring at 200 rpm for 30 min, the GA-MNP was removed and the concentration of copper ions in liquid solution was measured to estimate the amount of copper ions desorbed.

3. Results and discussion

3.1. Properties of gum arabic modified magnetic nano-adsorbent

According to our previous work, the mean diameter of MNP was about 13.2 nm [10]. However, the TEM image as shown in Fig. 2(a) indicated that GA-MNP had significantly larger particle size than MNP, revealing the modification with gum arabic resulted in the agglomeration of MNP. This might be due to the high molecular weight of gum arabic [8]. In spite of this, most of the resultant secondary particles still had smaller diameters in the range of 13–67 nm. The particle size distribution was indicated in Fig. 2(b), from which the mean diameter was estimated as 34.19 nm (±5.0%). The hydrodynamic diameter distribution of GA-MNP was indicated in Fig. 3. It was found that the hydrodynamic diameter distribution was 21.7–86.4 nm with the rest accounting for less than 1.0%. The mean hydrodynamic diameter was found to be 36.8 nm, in roughly agreement with the TEM image.

Both the XRD analysis of MNP and GA-MNP indicated six characteristic peaks at $2\theta = 30.1$, 35.5, 43.1, 53.4, 57.0, and 62.6°. They related to the (2 2 0), (3 1 1), (4 0 0), (4 2 2), (5 1 1), and (4 4 0) phases of Fe_3O_4, respectively, according to the database in JCPDS file (PCPDFWIN v.2.02, PDF no. 85–1436). This revealed that the resultant nanoparticles were pure Fe_3O_4 with a spinel structure. Also, the modification with gum arabic did not result in the phase change of Fe_3O_4.

The FTIR spectra of MNP, GA-MNP and gum arabic were shown in Fig. 4. The main characteristic peaks of gum arabic at 1049 and 1413 cm^{-1} (C–O stretch), 1612 cm^{-1} (C=O stretch and N–H bending), 2914 and 2995 cm^{-1} (C–H stretch), and 3000–3600 cm^{-1} (O–H stretch) were observed. As for the absorption band at 2360 cm^{-1}, it was usually due the CO_2 vibration. Noteworthily, although the presence of amine groups in gum arabic has been recognized [8], no significant and definite absorption bands for amine groups have been observed. Similar result was also obtained by Reis et al. [12]. The absorption band at 1612 cm^{-1} may be due to the C=O stretch and N–H bending, so it cannot be considered as a definite evidence for the presence of amine. Furthermore, the absorption bands due to the

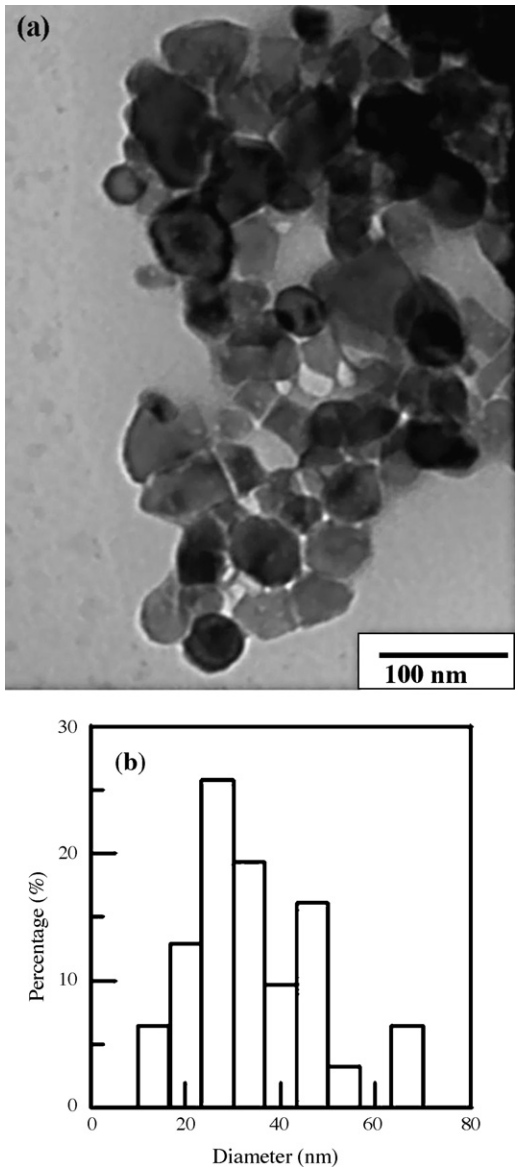

Fig. 2. Typical TEM image (a) and particle size distribution (b) of GA-MNP.

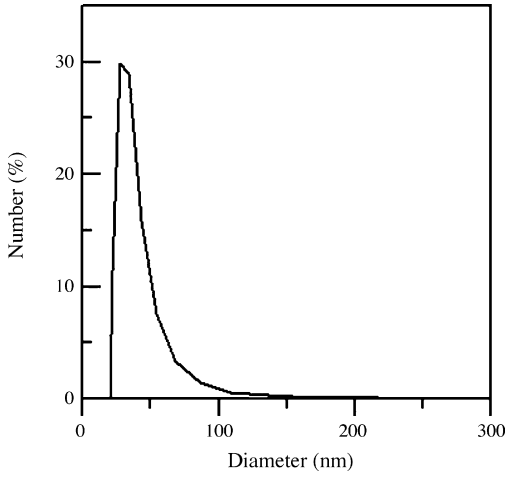

Fig. 3. Hydrodynamic diameter distribution of GA-MNP.

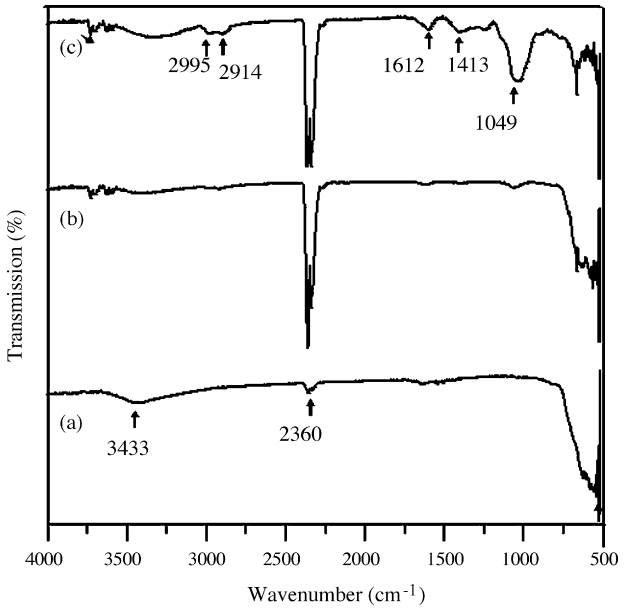

Fig. 4. FTIR spectra of MNP (a), GA-MNP (b) and GA (c).

N–H stretch for primary amine (usually at 3400–3500 cm^{-1}) and secondary amine (usually at 3310–3350 cm^{-1}) were also unobvious. However, it is known that gum arabic is made up of a high molecular weight glycoprotein and a lower molecular weight polysaccharide, and the amount of glycoprotein is less than that of polysaccharide [8]. So, the absorption bands due to the N–H stretch might be covered by the broad absorption band at 3000–3600 cm^{-1} due to the O–H stretch of polysaccharide. This might explain why no significant absorption bands due to the N–H stretch were observed in the FTIR spectra. In the case of MNP, the small absorption band at 2360 cm^{-1} should also be due to the CO_2 vibration. The broad absorption band at 3433 cm^{-1} indicated the presence of surface hydroxyl groups (O–H stretch). For the spectrum of GA-MNP, the significant absorption band at 2360 cm^{-1} was due to the CO_2 vibration as observed in the case of gum arabic. The small absorption band at 1049 cm^{-1} was due to the C–O stretch, revealing the binding of gum arabic on the surface of MNP. Furthermore, it was noted that the intensity of O–H stretch at 3433 cm^{-1} for GA-MNP was lower than that for MNP. Also, the other characteristic peaks of gum arabic at 1413, 1612 were too weak to be observed clearly. Both the facts suggested there was an interaction between the carboxylic groups of gum arabic and the surface hydroxyl groups of Fe_3O_4 nanoparticles [9]. This interaction also accounted for the mechanism of surface modification of MNP with gum arabic.

Since the surface charge state of gum arabic was quite different from that of Fe_3O_4 nanoparticles, the analysis of zeta potentials was further conducted to confirm the attachment of gum arabic surface onto the surface of Fe_3O_4 nanoparticles. Fig. 5 indicates the pH-dependences of zeta potentials for MNP and GA-MNP (0.1 mg/mL) in 0.01 M NaCl solutions at pH 1.70–11.0. Obviously, both the zeta potentials of MNP and GA-MNP nanoparticles increased with the decrease in pH due to the protonation of the hydroxyl groups on MNP or the carboxyl and amine groups of GA-MNP. It was obvious that the isoelectric

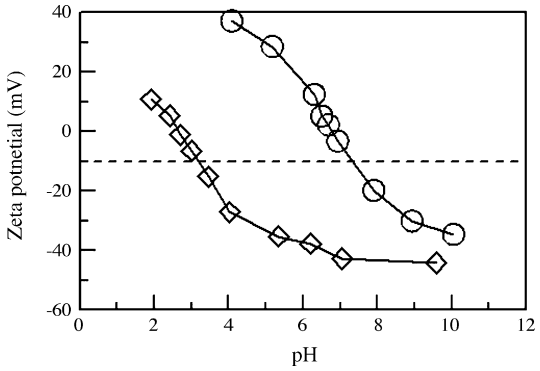

Fig. 5. Zeta potentials of MNP (◯) and GA-MNP (◊) at various pH values.

point (p_I) of MNP shifted from 6.78 to 3.60 after modification with gum arabic. This confirmed the attachment of gum arabic onto the surface of MNP and revealed that GA-MNP was positively charged at pH < 3.60.

To estimate the amount of gum arabic attached onto the surface of MNP, the thermogravimetric analysis of MNP and GA-MNP was conducted. As shown in Fig. 6, the TGA curve showed that the weight loss for MNP over the temperature range from 30 to 500 °C was only about 2.0%. This could be referred to the loss of residual water. On the other hand, for GA-MNP, the TGA curve showed two weight loss steps. The first weight loss step over the temperature range from 30 to 150 °C might be due to the loss of residual water in the sample. The weight loss in the region of 200–330 °C should be resulted by the decomposition of gum arabic. There was no significant weight change from 330 to 500 °C, implying the presence of only iron oxide within the temperature range. Accordingly, it was revealed that gum arabic indeed was attached onto the surface of MNP. Also, from the change of weight percentage in the TGA curves, it could be estimated that GA-MNP contained about 5.1% of gum arabic. Since the density of Fe_3O_4 is 5.18 g/cm^3 and the average molecular weight of gum arabic was about 2.5×10^5 [8], it could be estimated that averagely two gum arabic molecules were attached onto one Fe_3O_4 particle based on the assumption that the nanoparticles were spherical. Thus, the attachment of gum arabic onto the surface of MNP in this work was achieved at a molecular level.

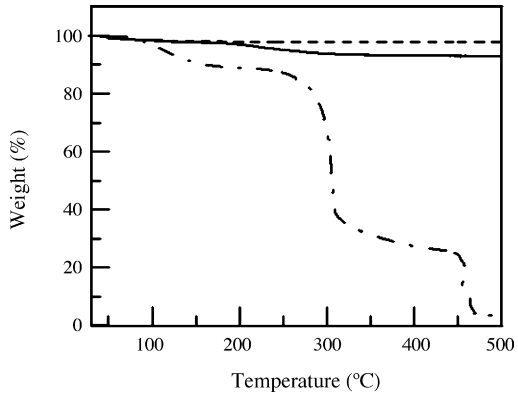

Fig. 6. TGA curves of MNP (-) and GA-MNP (–) and GA (–·–).

3.2. Effect of contact time on adsorption of copper ions

The feasibility of GA-MNP as a magnetic nano-adsorbent for the removal of heavy metal ions from aqueous solutions was demonstrated using copper ions as a model compound. The adsorption by MNP was also studied for comparison. First, the time required to achieve adsorption equilibrium was determined. The typical experiments were conducted at pH 5.1, 300 K, and an initial copper ion concentration of 200 mg/L. It was found that the adsorption equilibrium was reached within 2 min for both MNP and GA-MNP. Such a fast adsorption rate could be attributed to the external surface adsorption, which was different from the microporous adsorption process. Since nearly all the adsorption sites of MNP and GA-MNP existed on their exterior, it was easy for the adsorbate to access these active sites, thus resulting in a rapid approach to equilibrium.

3.3. Adsorption isotherms of copper ions

The equilibrium isotherms for the adsorption of copper ions by MNP and GA-MNP at pH 5.1 and 300 K were shown in Fig. 7. The equilibrium data were fitted by Langmuir and Freundlich isotherm equations [13,14]. The Langmuir equation can be expressed as:

$$\frac{C_e}{q_e} = \frac{C_e}{q_m} + \frac{1}{q_m K_L} \quad (1)$$

where q_e is the equilibrium adsorption capacity of copper ions on the adsorbent (mg/g), C_e the equilibrium copper ion concentration in solution (mg/L), q_m the maximum capacity of adsorbent (mg/g), and K_L is the Langmuir adsorption constant (L/mg). The linear form of Freundlich equation, which is an empirical equation used to describe heterogeneous adsorption systems, can be represented as follows:

$$\ln q_e = \ln K_F + \frac{1}{n} \ln C_e \quad (2)$$

where q_e and C_e are defined as above, K_F is Freundlich constant (L/mg), and n is the heterogeneity factor. The values of q_m and K_L were determined from the slope and intercept of the linear plots of C_e/q_e versus C_e (Fig. 8(a)) and of values of K_F and $1/n$ were determined from the slope and intercept of the linear plot of $\ln q_e$ versus $\ln C_e$ (Fig. 8(b)). It was found that the correlation coefficients of Langmuir isotherm were 0.9878 and 0.9982 for MNP and GA-MNP, respectively, and those for Freundlich isotherm were 0.9656 and 0.9036 for MNP and GA-MNP, respectively. This revealed the data were fitted better by Langmuir equation than by Freundlich equation. Thus, the adsorption of copper ions on the adsorbents obeyed the Langmuir adsorption isotherm. From the inset of Fig. 7, the q_m values for MNP and GA-MNP were estimated to be 17.6 and 38.5 mg/g, respectively, and the K_L values for MNP and GA-MNP were calculated as 0.013 and 0.012 L/mg. The adsorption capacity of GA-MNP for copper ions was comparatively higher than some of the polymer-based adsorbents recently reported. For example, the adsorption capacity of copper ions on the polystyrene-supported diethanolamine-typed dendrimer as reported by Sun et al. [15] was 20.73 mg/g, and those for the aminated polyacrylonitrile fibers and chitosan-bound Fe_3O_4 nanoparticles as reported by Deng et al. [16] and Chang et al. [17] were 31.45 and 21.50 mg/g, respectively.

In addition, Fig. 7 indicates obviously that GA-MNP was more effective in the removal of copper ions than MNP. The amount of copper ions adsorbed per gram of GA-MNP was more than twice that of MNP, revealing the modification with gum arabic indeed could enhance the adsorption capability. The corresponding adsorption mechanisms will be discussed later.

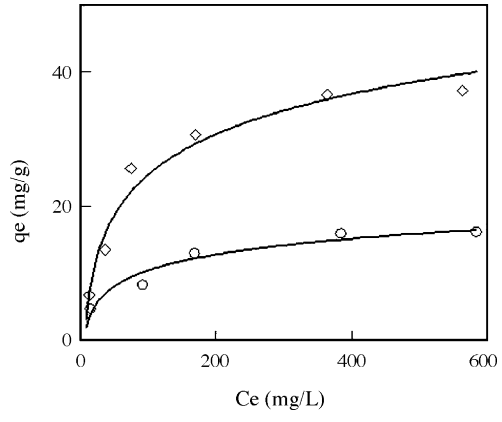

Fig. 7. Equilibrium isotherms for the adsorption of copper ions by MNP (◯) and GA-MNP (◊).

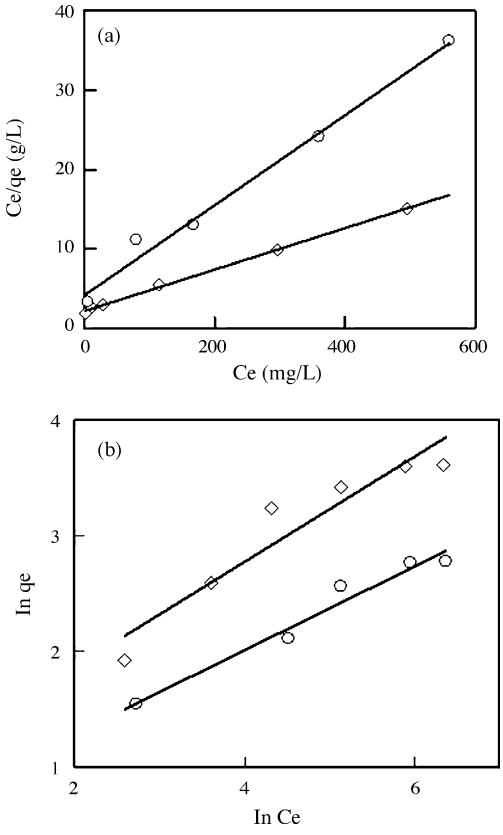

Fig. 8. Langmuir isotherm illustrating the linear dependences of C_e/q_e on C_e (a) and Freundlich isotherm illustrating the linear dependences of $\ln q_e$ on $\ln C_e$ (b).

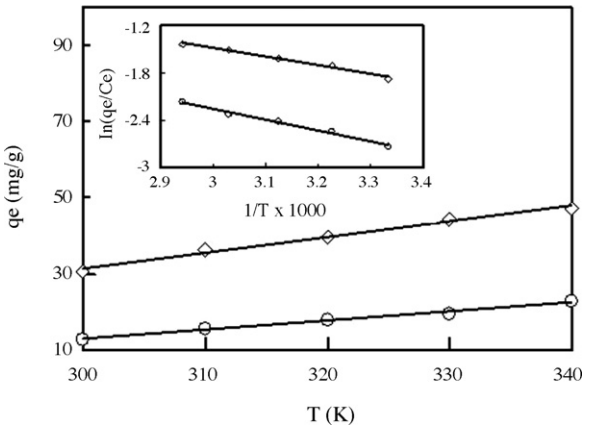

Fig. 9. Effects of temperature on the adsorption of copper ions by MNP (◯) and GA-MNP (◊). The inset is the plots of $\ln(q_e/C_e)$ against $1/T$ for MNP (◯) and GA-MNP (◊).

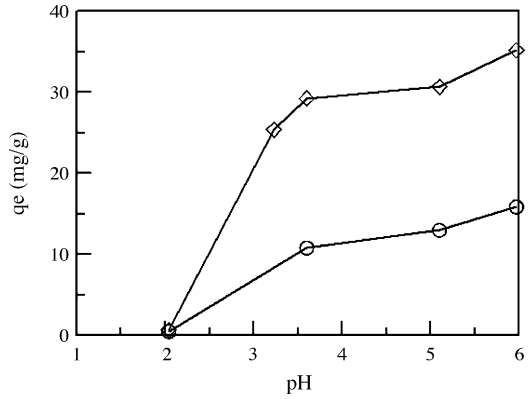

Fig. 10. Effects of solution pH on the adsorption of copper ions by MNP (◯) and GA-MNP (◊).

3.4. Effect of temperature on adsorption of copper ions

The effects of temperature on the adsorption of copper ions by MNP and GA-MNP were investigated at pH 5.1, 300–340 K, and an initial copper ion concentration of 200 mg/L. As shown in Fig. 9, the adsorption capacities for MNP and GA-MNP increased with the increase in temperature, revealing both the adsorption processes were endothermic. One possible explanation was that the metal ions were well hydrated. They have to lose part of hydration sheath in order to be adsorbed. This dehydration process of metal ions needed energy and superseded the exothermicity of the ion adsorption on the surface [18]. The plot of $\ln(q_e/C_e)$ versus $1/T$ was indicated in the inset of Fig. 9. From the slope ($-\Delta H/R$), the changes of enthalpy (ΔH) at 300–340 K could be determined to be 11.5 and 9.1 kJ/mol for MNP and GA-MNP.

In addition, the stability of GA-MNP magnetic nanoparticle at high temperature (340 K) was also studied by agitating the nanoparticle in distilled water for 60 min and then analyzing the amount of gum arabic present on the surface of MNP by TGA. It was found that the amount of gum arabic present on the surface of MNP after heat treatment had no significant loss, revealing the GA-MNP was highly stable in the examined temperature range.

3.5. Effect of pH on adsorption of copper ions

The effects of solution pH on the adsorption of copper ions by MNP and GA-MNP were investigated at pH 2–6, 300 K, and an initial copper ion concentration of 200 mg/L. As shown in Fig. 10, almost no adsorption of copper ions took place on MNP and GA-MNP when pH < 2, probably due to the significant competitive adsorption of hydrogen ions. At pH 2–6, the adsorption capacities increased with the increase in pH for both MNP and GA-MNP. Since the zeta potentials were positive at pH < 6.78 for MNP and pH < 3.60 for GA-MNP, the adsorption mechanisms for MNP and GA-MNP should be different and might be complex. Further discussion was given below. The adsorption studies at pH > 6 were not conducted because of the precipitation of $Cu(OH)_2$ from the solution [19].

3.5.1. Mechanism of copper ion adsorption on GA-MNP

The change in the adsorption characteristics with solution pH (Fig. 10) may be more clearly explained by the following equations, which depict the major characteristic reactions that can take place at the solid-solution interface of GA-MNP:

$$–NH_2 + H^+ = –NH_3^+ \quad (3)$$

$$–NH_2 + Cu^{2+} \rightarrow –NH_2Cu^{2+} \quad (4)$$

$$–NH_2 + OH^- = –NH_2OH^- \quad (5)$$

$$–NH_2OH^- + Cu^{2+}\ (\text{or } CuOH^+) = –NH_2OH^-\cdots Cu^{2+}(\text{or } –NH_2OH^-\cdots CuOH^+) \quad (6)$$

The protonation and deprotonation reactions of the amine groups of GA-MNP in the solution was indicated by Eq. (3). Eq. (4) shows the formation of surface complexes of copper ions with the amine groups, and Eq. (5) describes the adsorption of OH^- ions from the solution through hydrogen bond at high pH values [20]. The reaction in Eq. (3) favored the protonation of the amine groups to form $–NH_3^+$ at lower pH values. With the conversion of more $–NH_2$ groups to $–NH_3^+$, there were only fewer $–NH_2$ sites available on the GA-MNP surface for Cu^{2+} adsorption through Eq. (4). Moreover, the electrostatic repulsion between the Cu^{2+} and the surfaces of the GA-MNP increased with the formation of more $–NH_3^+$ sites on the surface. All these effects would result in the reduction of Cu^{2+} adsorption on the GA-MNP with decreasing solution pH values. On the other hand, with the increase of solution pH, the reaction in Eq. (3) proceeded to the left, resulting in an increase of the number of $–NH_2$ sites on the surface of GA-MNP for copper ion adsorption through Eq. (4), thus increasing the adsorption capacity. At higher solution pH, the reaction in Eq. (5) might proceed. This reaction on one hand could reduce the adsorption of copper ions through surface complexation in Eq. (4), but on the other hand might increase the adsorption of copper ions through the electrostatic attraction as indicated in Eq. (6).

3.5.2. Mechanism of copper ion adsorption on MNP

The most abundant surface functional group participating in the reactions on oxide surfaces is the hydroxyl group, which is amphoteric and reactive. Depending on the solution pH, the oxide surface can act as a weak acid or base and gain or lose proton (i.e., it can undergo protonation or deprotonation) [2]. Therefore, the following reactions are expected to occur at the surface of MNP in the pH region of 2.0–6.0.

$$–FeO^- + H^+ = –FeOH \quad (7)$$

$$–FeOH + H^+ = –FeOH_2{}^+ \quad (8)$$

where FeOH represents a singly protonated oxide site. The above reactions revealed that increasing the concentration of deprotonated surface oxide sites increased the adsorption capacity of cations that proposed to occur according to the following reactions.

$$–m\text{FeOH} + Cu^{2+} = –(\text{Fe–O})_m Cu^{(2-m)+} + mH^+ \quad (9)$$

where –FeOH is the surface hydroxyl site. At low pH, $–FeOH_2{}^+$ is the dominating surface species and hence the surface has high positive charge density which make the adsorption of copper ions unfavorable due to the strong electrostatic repulsion. So, almost no copper ions were adsorbed at pH ≤ 2. With increasing pH, zeta potential decreased and –FeOH became the dominating species. Thus, the removal of copper ions from the aqueous solution could be achieved through an ion exchange process as shown in Eq. (9).

3.6. Desorption and reusability studies

For potential practical applications, the regeneration and reuse of an adsorbent are important. From the pH study, it has been found that the adsorption of copper ions on GA-MNP at pH ≤ 2.0 was negligible. This suggested that desorption of copper ions from GA-MNP was possible around pH 2.0. Therefore, HCl solutions of different pH (3.0, 2.0 and 1.5) were used to examine the desorption study. It was found that the desorption percentages were 81, 92, and 93% in the HCl solutions of pH 3.0, 2.0, and 1.5, respectively. The higher desorption efficiency at lower pH value could be referred to the sufficiently high hydrogen ion concentration, which led to the strong competitive adsorption.

The reusability of GA-MNP as an adsorbent was also studied after the desorption process. The reusability was checked by following the adsorption–desorption process for three cycles and the adsorption efficiency in each cycle was analyzed. The adsorption process was followed by shaking 25 mg of GA-MNP in 5 mL of 200 mg/L copper ion solution at pH 5.10 for 5 min at 200 rpm. The desorption study was conducted in the HCl solution at pH 2.0 as mentioned above. It was found that the adsorption capacities were 28.12, 27.64 and 27.18 mg/g in the first, second and third adsorption–desorption cycles, respectively. Thus, the GA-MNP adsorbent can be reused almost without any significant loss in the adsorption performance.

4. Conclusions

A novel magnetic nano-adsorbent was fabricated by modifying the surface of Fe_3O_4 nanoparticles with gum arabic. The TEM, DLS, and XRD analysis indicated the surface modification resulted in the agglomeration of Fe_3O_4 nanoparticles to form the secondary particles with diameters in the range of 20–50 nm, which did not change the spinel structure of Fe_3O_4. FTIR analysis demonstrated the attachment of gum arabic on the surface of Fe_3O_4 nanoparticles was achieved via the interaction between the carboxylic groups of gum arabic and the surface hydroxyl groups of Fe_3O_4. Zeta potential analysis confirmed the binding of gum arabic on the surface of Fe_3O_4 nanoparticles and revealed the shift of isoelectric point from 6.80 to 3.60 after surface modification. With the help of TGA analysis, the amount of gum arabic in the final product was determined to be about 5.1 wt%. Further calculation indicated the binding was achieved at a molecular level, averagely two gum arabic molecules were bound to one Fe_3O_4 particle. Both MNP and GA-MNP were quite efficient as a magnetic nano-adsorbent for the fast removal of copper ions from aqueous solutions due to high specific surface area and the absence of internal diffusion resistance. The time required to achieve the adsorption equilibrium was only 2 min. The adsorption capacity of GA-MNP was significantly higher than that of MNP, and the adsorption capacities for both MNP and GA-MNP increased with the increase of solution pH. The adsorption of copper ions on the surface of GA-MNP could be attributed to the surface complexation because of the presence of amine groups of gum arabic, while the adsorption on the surface of MNP was mainly resulted by the surface hydroxyl groups of iron oxide. Both the adsorption data followed the Langmuir isotherm equation. The maximum adsorption capacities and Langmuir adsorption constants were 17.6 mg/g and 0.013 L/mg for MNP and 38.5 mg/g and 0.012 L/mg for GA-MNP, respectively. Because of the dehydration of hydrated metal ions, the adsorption process was endothermic with the enthalpy changes of 11.5 and 9.1 kJ/mol for MNP and GA-MNP, respectively. In addition, acid solutions at pH ≤ 2 was suitable for the desorption of copper ions and the reusability of GA-MNP was good. This novel product should be useful for the fast removal of heavy metal cations.

References

[1] Y. Mido, M. Satake, Chemicals in the Environment, Discovery Publishing House, New Delhi, 1995.
[2] S.S. Banerjee, R.V. Jayaram, M.V. Joshi, Removal of Cr(VI) and Hg(II) from aqueous solutions using fly ash and impregnated fly ash, Sep. Sci. Technol. 39 (2004) 1611–1629.
[3] H.S. Murlidhara, Advances in Solid–Liquid Separation, Batelle Press, Colombus Richland, Ohio, 1986.
[4] M. Weltrowski, B. Martel, M. Morcellet, Chitosan *N*-benzyl sulfonate derivatives as sorbents for removal of metal ions in an acidic medium, J. Appl. Polym. Sci. 59 (1996) 647–654.
[5] R.W. Siegel, E. Hu, M.C. Roco, Nanostructure Science and Technology, A Worldwide Study, WTEC, Loyola College Kluwer Academic, Baltimore, MD, 1999.
[6] A. Ngomsik, A. Bee, M. Draye, G. Cote, V. Cabuil, Magnetic nano and microparticles for metal removal and environmental applications: a review, C. R. Chimie. 8 (2005) 963–970.

[7] G.F. Goya, T.S. Berquo, F.C. Fonseca, Static and dynamic magnetic properties of spherical magnetite nanoparticles, J. Appl. Phys. 94 (2003) 3520–3528.
[8] E.V. Groman, E.T. Menz, P.M. Enriquez, C. Jung, J.M. Lewis, L. Josephson, Delivery of therapeutic agents to receptors using polysaccharides, United States Patent, 5554386, 1996.
[9] Y.K. Leong, U. Seah, S.Y. Chu, B.C. Ong, Effect of gum arabic macromolecules on surface forces in oxide dispersion, Coll. Surface 182 (2001) 263–268.
[10] M.H. Liao, D.H. Chen, Preparation and characterization of novel magnetic nano-adsorbents, J. Mater. Chem. 12 (2002) 3654–3659.
[11] S.Y. Mak, D.H. Chen, Binding and sulfonation of poly(acrylic acid) on iron oxide nanoparticles: a novel, magnetic, strong acid cation nano-adsorbent, Macromol. Rapid Commun. 26 (2005) 1567–1571.
[12] A.V. Reis, M.R. Guilherme, O.A. Cavalcanti, A.F. Rubira, E.C. Muniz, Synthesis and characterization of pH-responsive hydrogels based on chemically modified arabic gum polysaccharide, Polymer 47 (2006) 2023–2029.
[13] S.S. Banerjee, M.V. Joshi, R.V. Jayaram, Treatment of oil spills using organo-fly ash, Desalination 195 (2006) 32–39.
[14] Y.C. Chang, D.H. Chen, Adsorption kinetics and thermodynamics of acid dyes on a carboxymethylated chitosan-conjugated magnetic nano-adsorbent, Macromol. Biosci. 5 (2005) 254–261.
[15] C. Sun, R. Qu, C. Ji, C. Wang, Y. Sun, Z. Yue, G. Cheng, Preparation and adsorption properties of crosslinked polystyrene-supported low-generation diethanolamine-typed dendrimer for metal ions, Talanta 70 (2006) 14–19.
[16] S. Deng, R. Bai, J.P. Chen, Aminated polyacrylonitrile fibers for lead and copper removal, Langmuir 19 (2003) 5058–5064.
[17] Y.C. Chang, D.H. Chen, Preparation and adsorption properties of monodisperse chitosan-bound Fe_3O_4 magnetic nanoparticles for removal of Cu(II) ions, J. Colloid Interface Sci. 283 (2005) 446–451.
[18] R. Naseem, S.S. Tahir, Removal of Pb(II) from aqueous/acidic solutions by using bentonite as an adsorbent, Water Res. 35 (2001) 3982–3986.
[19] M.Y. Pamukoglu, F. Kargi, Removal of copper(II) ions from aqueous medium by biosorption onto powdered waste sludge, Process Biochem. 41 (2006) 1047–1054.
[20] L. Jin, R.B. Bai, Mechanisms of lead adsorption on chitosan/PVA hydrogel beads, Langmuir 18 (2002) 9765–9770.